Published in final edited form as:
J Neurochem. 2008 July ; 106(2): . doi:10.1111/j.1471-4159.2008.05451.x.

REGULATION OF NEURAL PROGENITOR CELL MOTILITY BY CERAMIDE AND POTENTIAL IMPLICATIONS FOR MOUSE BRAIN DEVELOPMENT

Guanghu Wang, **Kannan Krishnamurthy**, **Ying-Wei Chiang**, **Somsankar Dasgupta**, and **Erhard Bieberich**
Program in Developmental Neurobiology, Institute of Molecular Medicine and Genetics, School of Medicine Medical College of Georgia, Augusta, GA 30912

Abstract

We provide evidence that the sphingolipid ceramide, in addition to its pro-apoptotic function, regulates neural progenitor (NP) motility *in vitro* and brain development *in vivo*. Ceramide (N-palmitoyl D-erythro sphingosine and N-oleoyl D-erythro sphingosine) and the ceramide analog N-oleoyl serinol (S18) stimulate migration of NPs in scratch (wounding) migration assays. Sphingolipid depletion by inhibition of *de novo* ceramide biosynthesis, or ceramide inactivation using an anti-ceramide antibody, obliterates NP motility, which is restored by ceramide or S18. These results suggest that ceramide is crucial for NP motility. Wounding of the NP monolayer activates neutral sphingomyelinase indicating that ceramide is generated from sphingomyelin. In membrane processes, ceramide is co-distributed with its binding partner atypical PKζ/λ (aPKC), and Cdc42, α/β-tubulin, and β-catenin, three proteins involved in aPKC-dependent regulation of cell polarity and motility. Sphingolipid depletion by myriocin prevents membrane translocation of aPKC and Cdc42, which is restored by ceramide or S18. These results suggest that ceramide-mediated membrane association of aPKC/Cdc42 is important for NP motility. *In vivo*, sphingolipid depletion leads to ectopic localization of mitotic or post-mitotic neural cells in the embryonic brain, while S18 restores the normal brain organization. In summary, our study provides novel evidence that ceramide is critical for NP motility and polarity *in vitro* and *in vivo*.

Keywords

ceramide; sphingolipids; motility; brain morphogenesis; polarity

INTRODUCTION

In neural cells, the regulation of cell polarity, adhesion, and motility critically relies on atypical PKCζ/λ (aPKC) and a group of associated proteins such as Par3, Par6, Cdc42, GSK-3β, and β-catenin (Etienne-Manneville and Hall 2001; Kay and Hunter 2001; Ohno 2001; Etienne-Manneville and Hall 2002). In particular, a complex consisting of aPKC, Par3, Par6, and Cdc42 has been implicated in converting the activation of aPKC into the stabilization or localized membrane translocation of microtubules or β-catenin, respectively (Etienne-Manneville and Hall 2001, 2003a, b; Liu et al. 2004; Liu et al. 2006). Consistently, the phenotype of aPKC deficiency in zebrafish and mouse demonstrates that aPKC plays a

Address correspondence to: Erhard Bieberich Institute of Molecular Medicine and Genetics Medical College of Georgia 1120 15th Street Room CB-2803 Augusta, GA 30912 Phone: 706-721-9113 Fax: 706-721-8685 ebieberich@mcg.edu.

key role in embryo development and adherens junction formation (Horne-Badovinac et al. 2001; Soloff et al. 2004; Koike et al. 2005; Imai et al. 2006).

Conditional knockout of aPKC, Cdc42 and β-catenin in neural progenitors (NPs) results in remarkably similar phenotypes of aberrant mouse brain development characterized by: (1) loss of adhesion and detachment of NPs from the neuroepithelium concurrent with disrupted interkinetic nuclear migration and ectopic localization of post-mitotic neuronal precursors, and (2) disturbed morphogenesis of the cortical plate and lamination of the neocortex (Machon et al. 2003; Cappello et al. 2006; Chen et al. 2006; Imai et al. 2006). These studies show that aPKC and its associated proteins are crucial in regulating neural cell polarity and embryonic brain development. However, it is not fully understood which factor(s) activate(s) aPKC and initiate(s) the formation of the aPKC-associated protein complex.

We and others have shown that ceramide: (1) activates aPKC at low concentration (Lozano et al. 1994; Muller et al. 1995; Wang et al. 1999; Bieberich et al. 2000; Bourbon et al. 2000; Wang et al. 2005) especially in NPs (Wang et al. 2005); (2) recruits aPKC to structured membrane microdomains in rat smooth muscle cells or adipocytes (Fox et al. 2007; Hajduch et al. 2007), and (3) translocates aPKC to the apicolateral cell membrane in primitive ectoderm cells (Krishnamurthy et al. 2007b)(see Supplemental Fig. 1 for structure of ceramide). NPs are self-renewing, multipotent cells that can differentiate into either neurons or glial cells. In the developing mouse brain, NPs in the neuroepithelium differentiate into more committed (neuronal) precursor cells that migrate from the ventricular zone (VZ) to the superficial layers of the cortical plate (CP) forming the six-layered neocortex (Hatten 1999; Marin and Rubenstein 2003). Atypical PKC and its associated protein complex regulating cell adhesion and motility are indispensable for this process (Etienne-Manneville and Hall 2001; Ohno 2001; Imai et al. 2006; Welchman et al. 2007). Therefore, ceramide may play an important role in activating aPKC or priming its association with other proteins, which regulates NP motility and adhesion.

To investigate this potential function of ceramide, we incubated NPs with various ceramide species or analogs and quantified cell motility in scratch migration assays. We also inhibited *de novo* ceramide biosynthesis in NPs and *in vivo*, in mouse embryos using myriocin (ISP-1), a specific serine palmitoyltransferase (SPT) inhibitor, or fumonisin B1 (FB1), a ceramide synthase inhibitor (Chalfant et al. 2002; He et al. 2004). Our results show that ceramide or ceramide analog (N-oleyl serinol or S18, Supplemental Fig. 1)) incubation resulted in enhanced motility, while sphingolipid depletion resulted in reduced motility of NPs *in vitro*. *In vivo*, sphingolipid depletion caused molecular and phenotypic characteristics of NP-specific conditional knockout mice for aPKC, Cdc42 and β-catenin. Ceramide and S18 rescued the migratory phenotype of NPs and restored brain morphology. This data suggests that ceramide is an essential regulator of the formation of aPKC-dependent protein complexes controlling NP motility and embryonic brain development.

MATERIALS AND METHODS

Materials

Embryonic stem (ES)-J1 mouse ES cells and feeder cells were obtained from the ES cell core facility (Dr. A. Eroglu, Medical College of Georgia, Augusta, GA) and characterized as described previously (Bieberich et al. 2003). C17.2 mouse NPs were a generous gift from Dr. Evan Snyder (Harvard Medical School, Boston, MA). Rabbit polyclonal anti-ceramide IgG was prepared as described previously (Krishnamurthy et al. 2007a). Topro-3-iodide, Amplex Red sphingomyelinase assay, and FGF-2 were from Invitrogen (Carlsbad, CA). DMEM/Ham's F-12 50/50 mix was purchased from Cellgro (Herndon, VA). ESGRO, leukemia inhibitory factor (LIF), and Tuj1 (β-tubulin III) antibody were from Chemicon

International (Temecula, CA). Hoechst 33258, myriocin, horseradish peroxidase-conjugated goat anti rabbit IgG, and anti-lysenin rabbit IgG were from Sigma-Aldrich (St. Louis, MO). Fumonisin B1 (FB1) was from Alexis Biochemicals (San Diego, CA). Mouse monoclonal anti-GSK-3α/β, and rabbit polyclonal anti-PKCζ/λ antibody were from Santa Cruz (Santa Cruz, CA). Rabbit polyclonal anti-phospho-serine 9 GSK-3β and β-catenin antibody were from Cell Signaling Technologies (Beverly, MA). Mouse polyclonal anti-ceramide IgM MAS0020 was from Kuekels Biotech (Kuekels, Germany). Cy2-conjugated anti-mouse IgM (μ-specific), Cy3-conjugated anti-mouse IgG (γ-specific) and Cy5-conjugated anti-rabbit IgG were from Jackson Immunochemicals (West Grove, PA). Rabbit anti-phospho-histone 3 (pH3) antibody was from Upstate (Charlottesville, VA). Lysenin was obtained from Peptides International (Louisville, KY). C2, C8, C16:0, and C18:1 D-*erythro* ceramide was from Avanti Polar Lipids (Alabaster, AL). All reagents used were of analytical grade or higher.

ES cells, cultivation and differentiation, and scratch migration assay

The *in vitro* neural differentiation of mouse ES cells (ES-J1) was performed as described before (Bieberich et al. 2004; Wang et al. 2005). The NPs were cultivated until reaching more than 90% confluence (about 72 h after re-plating of dissociated embryoid bodies (EBs)). A gap of 200 μm width was generated by removing NPs using a pair of sterilized tweezers and migration monitored by taking micrographs at different time points. Five μM myriocin or 20 μM FB1 were added 24 hours after NPs were plated. At these concentrations, ceramide levels in NPs were reduced by 50% (EC50 for myriocin = 3 μM) or more. One μM C16:0 or C18:1 ceramide (pre-dissolved as 1000x stock solution in 2% dodecane/ethanol), 40 μM S18, or 20 μM LiCl were added 1 hour before generating the gap (all concentrations were final). The distance (D) between the cells on both sides of the gap was measured. The average velocity was calculated using the equation: $v=(D_0-D_t)/2t$, where v is velocity (μm/h); t is time (h); D_0 is the distance at time zero (μm); and D_t is the distance at time t (μm). At least 100 representative areas along the axis of the scratch were measured for each experiment. Each experiment was repeated 3 times (n = 3) starting with independent C17.2 or ES cell batches. Means and standard deviations were determined as described in Statistics. Differentiation to neuronal precursors was induced by further cultivating NPs in differentiation medium (Neurobasal with 5% serum and B27 supplement). FGF-2 was withdrawn from the medium and cells were grown for another 24-48 hours. Myriocin (5 μM) was added at day 3 of NP culture and then further incubated until the cells were collected or fixed.

Statistics

Means, standard deviation, and standard error of the means were calculated using Microsoft Excel. Student's *t*-test was used for testing significance. $P<0.05$ was considered statistically significant.

Immunocytochemistry and image analysis

Immunostaining of fixed NPs followed procedures described previously (Wang et al. 2005). Non-specific antigen binding sites were saturated by incubation with 3% ovalbumin, 2% donkey serum in PBS. For ceramide staining, the specimens were first incubated with ceramide antibody without permeabilization. Sphingomyelin (SM) was detected by first incubating fixed cells with lysenin (1 μg/ml) in 0.1% ovalbumin/ phosphate-buffered saline (PBS) (Yamaji et al. 1998; Hullin-Matsuda and Kobayashi 2007). The specimens were then fixed again and permeabilized with 0.2% Triton X-100/PBS, 5 min at room temperature) for immunostaining of intracellular proteins. Epifluorescence microscopy was performed with an Axiophot microscope (Carl Zeiss MicroImaging, Inc.) equipped with a Spot II CCD camera. Confocal fluorescence microscopy was performed using a Zeiss LSM confocal laser

scanning microscope equipped with a two-photon argon laser at 488 nm (Cy2), 543 nm (Cy3, Alexa Fluor® 546), or 633 nm (Cy5, Alexa Fluor® 647), respectively. Phase contrast micrographs and live cell imaging were taken using Nikon Eclipse TE300 (Japan). Micrographic images were taken at the same settings for laser intensity, pinhole, and signal amplification. Images obtained with secondary antibody only were used as negative controls representing the background intensity in a particular laser channel. Pixels with at least double the background intensity were considered significant and counted as (+) value. All others were counted as (−) value. Counting was performed with at least five fields on each section or slide and at least 50 cells in each field from at least 4 independent samples (n=4).The statistical significance of the co-distribution of two signals was calculated using Chi square analysis following published procedures (Bieberich et al. 2003; Bieberich et al. 2004). A value of $P<0.05$ was considered statistically significant.

Lipid analysis and nSMase assay

Total lipids were extracted from NPs as described previously (Bieberich et al. 2001; Wang et al. 2005). Lipids were separated by high-performance thin-layer chromatography (HPTLC) using the running solvents $CHCl_3$:CH_3OH:CH_3COOH (95:4.5:0.5; v/v) for the resolution of individual lipid bands. Lipids were stained with the cupric acetate/sulfuric acid reagent and the identity of the ceramide band was confirmed by alkaline hydrolysis of phospholipids followed by silicic acid chromatography using a protocol as previously published (Dasgupta and Hogan 2001). For gas chromatography-mass spectrometry (GC-MS) analysis, ceramide isolated by silic acid chromatography and preparative TLC was methanolyzed at 80 °C in methanol/HCl for 18 h. The reaction product was partitioned three times with equal volumes of hexane to separate fatty acid methyl esters. The hexane phases (fatty acid methyl esters) were combined and injected into a 5980 Hewlett Packard GC instrument equipped with a 5972 MS device. The fatty acid methyl esters were identified by retention time and mass spectrometry (MS) by comparison with standard lipids (Supplemental Fig. 2). The enzyme activity of neutral sphigomyelinase (nSMase) was determined using the fluorimetric Amplex Red assay and 50-100 μg cellular protein following the manufacturer's protocol (Invitrogen).

Subcellular fractionation and co-immunoprecipitation assay

Cells were trypsinized, rinsed twice with ice-cold PBS, re-suspended in HEPES-sucrose buffer containing 250 mM sucrose, 10 mM HEPES buffer (pH 7.4), 2 mM magnesium chloride, 1 mM each of EDTA, EGTA and PMSF (with protease and phosphatase inhibitors added, before use), and homogenized using a Dounce glass homogenizer. The subcellular fractionation was performed by sequential centrifugation, with the final step at 110,000×g for 90 min to obtain the cytosolic fraction (supernatant) and the membrane fraction (pellet). All centrifugation steps were carried out at 4 °C. The protein from the cytosolic fraction was concentrated by chloroform-methanol (Wessel-Flugge) precipitation (Wessel and Flugge 1984). Equal amounts of protein from each fraction were applied to SDS gel electrophoresis and immunoblotting. Equal loading was confirmed by reversible staining of the transferred proteins with Ponceau S. Co-immunoprecipitation assays were performed as described previously (Krishnamurthy et al. 2007b).

Animal care and treatment

C57CLB6 mice were housed and treated at the Laboratory Animal Service of the Medical College of Georgia following approved protocols. For timed pregnancy, the morning of vaginal plug detection was designated as gestational day E0.5. Myriocin was administered three times into pregnant mice by intraperitoneal (i.p.) injection at a dose of 1 mg/kg body weight on days E11.5, E13.5 and E15.5. For the S18 rescue experiment, the myriocin-injected mice were further i.p. injected with S18 at a dose of 25 mg/kg body weight on day

E12.5, E14.5 and E16. The mice were sacrificed on day E16.5 and embryos were frozen for protein and lipid analysis, or they were fixed overnight in 4% paraformaldehyde, rinsed extensively in PBS, and cryoprotected in 30% sucrose before sectioning (sagittal) at 7 μm thickness using a cryostat instrument. Four independent samples were taken with each sample yielding 60-80 sections. Myriocin and S18 were first dissolved in DMSO as a stock solution. Before injection, they were diluted at least 10 times with PBS, and 100 μl myriocin (25 μg) or 50 μl S18 (625 μg) injected into the pregnant mice. Control mice received vehicle of equivalent composition, but without myriocin or S18.

Descriptions of videos

Time lapse photographs were taken every 10 minutes immediately after generating the gap in a scratch migration assay using a microscope equipped with an environmental chamber that was equilibrated to 37 °C and 5% CO2 atmosphere. **Video A**, control NPs. **Video B**, myriocin treated NPs.

RESULTS

Ceramide is essential for NP motility

To test the effect of ceramide on cell motility we incubated C17.2 cells, an immortalized, well-established murine NP cell line (Kitchens et al. 1994; Riess et al. 2002), with 1 μM of C16:0 or C18:1 ceramide (N-palmitoyl or N-oleoyl sphingosine, see Supplemental Fig. 1). Using GC-MS we found that these were the two major ceramide species synthesized in C17.2 cells (GC-MS data in Supplemental Fig. 2). The effect of ceramide on cell motility was determined by monitoring the migration of C17.2 cells into a 200 μm wide gap within a time period of 6 h (scratch wounding or migration assay). Figure 1A shows that C16:0 or C18:1 ceramide increased the velocity of migration by about 70% from 14.5+/−2.0 μm/h to 24.1+/−2.6 or 25.5+/−2.3 μm/h, respectively. A similar effect was observed for the C18:1 ceramide analog N-oleoyl serinol (S18, Fig. 1A and Supplemental Fig. 1), which was, for the first time, synthesized and characterized in our laboratory (Bieberich et al. 2000; Bieberich et al. 2002; Bieberich et al. 2004). The velocity increase was already detectable within the first 2 h of incubation indicating that this effect of ceramide or S18 did not rely on altered gene or protein expression, or alternative splicing as observed for other ceramide effects (Chalfant et al. 2002). There was no velocity increase when short-chain C2 ceramide was used, suggesting that the ceramide effect was specific for the endogenous ceramide species (Fig. 1A).

To test whether sphingolipid depletion affected the motility of NPs we incubated the cells with two sphingolipid biosynthesis inhibitors (myriocin or fumonisin B1 (FB1)) and quantified the number and velocity of migrating NPs. In addition to C17.2 cells, we used embryonic stem (ES) cell-derived NPs that were generated following an established differentiation protocol (Bieberich et al. 2004; Wang et al. 2005; Krishnamurthy et al. 2007b). Quantitative high-performance thin-layer chromatography (HPTLC) showed that myriocin treatment for 48 h significantly reduced ceramide levels in C17.2 cells or ES cell-derived NPs (to 31 or 36% of controls; Fig. 1B). A similar result, although less dramatic, was obtained with FB1 (Fig. 1B, right panel). The identity of the ceramide band was confirmed by alkaline hydrolysis of phospholipids followed by silicic acid chromatography.

The scratch migration assay showed that myriocin treatment significantly reduced the velocity of C17.2 cells to an average speed of 4.0+/−2.2 μm/h (Fig. 1A) and that of ES cell-derived NPs to 4.7+/−1.5 μm/h. This corresponded well to the extent of ceramide reduction with myriocin (Fig. 1B). Likewise, reduction of motility with FB1 (to 8.4+/−1.1 μm/h for ES cell-derived NPs) was directly correlated with the extent of ceramide reduction (Fig. 1B).

We then determined whether sphingolipid depletion affected the number of migrating NPs. Figure 1C shows that after incubation with myriocin, the number of cells that migrated over a distance of more than 50 μm decreased by more than 90%. The number of TUNEL-positive NPs was not elevated by myriocin or FB1, demonstrating that this effect was not caused by increased cell death. The dramatically reduced motility of NPs after sphingolipid depletion was also demonstrated by time-lapse video microscopy (Supplemental videos A and B).

To determine whether the effect of myriocin treatment was dependent on the depletion of ceramide itself and not on a ceramide derivative, we attempted to rescue cell motility by adding back different ceramide species and analogs to the myriocin-incubated cells. In C17.2 cells, C16:0 ceramide (1 μM), C18:1 ceramide (1 μM), S18 (40 μM) and endogenous ceramide (0.25 μg/ml purified from C17.2 cells), but not C2:0 ceramide (N-acetyl sphingosine, 15 μM) or C8:0 ceramide (N-octyl sphingosine, 5 μM) restored migration of myriocin-treated cells (Fig. 1A). The ceramide derivative sphingosine-1-phosphate (S1P, 1 μM) did not restore migration of myriocin-incubated NPs. We also tested the effect of inhibiting glycolipid biosynthesis with N-butyl deoxinojirimycin (200 μM) on cell motility, but we did not find a significant difference to control NPs. Therefore, our data suggested that myriocin (or FB1)-induced reduction of NP motility was most likely due to ceramide depletion, which was rescued by C16 ceramide, C18:1 ceramide, endogenous ceramide, and S18.

The function of ceramide as the regulatory factor required for NP motility was further analyzed using a novel anti-ceramide antibody (rabbit IgG) that has been generated and characterized in our laboratory (Krishnamurthy et al. 2007a). Ceramide can be rapidly flipped between the outside and inside of the cell membrane (Lopez-Montero et al. 2005). Therefore, an anti-ceramide antibody can trap ceramide at the outside when added to the cell culture medium. As a result, aPKC will not have access to ceramide as binding partner at the inner leaflet and it will re-distribute to other compartments. Fig. 2 and Supplemental Fig. 3 show that incubation with anti-ceramide rabbit IgG changed the morphology of C17.2 cell and ES cell-derived NPs by reducing the formation of membrane protrusions and lamellipodia. Often, cells were rounded up or formed clusters (Fig. 2 and Supplemental Fig. 3) suggesting that the anti-ceramide rabbit IgG affected the dynamics of the cytoskeleton. The effect of the anti-ceramide rabbit IgG was confirmed using a different, commercially available antibody against ceramide (mouse IgM MAS0020 (Vielhaber et al. 2001; Cowart et al. 2002)). Removal of the anti-ceramide antibodies from the medium restored membrane protrusions, indicating that the effect on the cytoskeleton was reversible. Non-specific (pre-immuneserum) rabbit IgG, an antibody (protein A sepharose-enriched rabbit IgG fraction) against an unrelated cell surface lipid (GA1) and rabbit IgG against a surface protein (fibroblast growth factor receptor 1) did not induce alteration of the cell shape or motility, confirming the specificity of the effect of the anti-ceramide antibody.

Using immunocytochemistry for aPKC and cytoskeletal proteins we tested if inactivation of ceramide on the cell surface affected the membrane translocation of aPKC and the formation of microtubules and F-actin. Fig. 2A and B shows that C17.2 cells incubated with control IgG formed numerous membrane protrusions and lamellipodia that co-distributed with aPKC, α-tubulin and F-actin (arrows). Incubation with the anti-ceramide IgG induced a rapid change of the aPKC distribution from the plasma membrane to the cytosol and nucleus (Fig. 2C). Loss of membrane-bound aPKC was concomitant with retraction of microtubules and membrane processes, which resulted in the formation of round-shaped cells that showed no or only low motility. Most remarkably, the addition of C16 ceramide or S18 to the medium prevented the effect of the antibody (Fig. 2D and Supplemental Fig. 3). S18 was not recognized or trapped by the anti-ceramide antibody. Hence, it was able to mimic the

function of ceramide and keep aPKC at the membrane despite of endogenous ceramide being trapped at the outside. Taken together, this data suggested that ceramide mediates membrane association of aPKC, which is required for NP motility.

Elevation of ceramide triggers microtubule-associated process formation and recruits polarity proteins to the cell membrane

The effect of exogenous C16 ceramide, C18:1 ceramide, and S18 on the stimulation or restoration of cell motility, process formation, and microtubule extension suggested that ceramide was released at the cell membrane. It is known that membrane-resident ceramide can be generated by hydrolysis of sphingomyelin (SM, for structure see Supplemental Fig. 1), a reaction catalyzed by neutral sphingomyelinase (nSMase) (Clarke and Hannun 2006; Clarke et al. 2006). We assayed the scratch-induced activation of nSMase and used immmunocytochemistry to determine the distribution of SM and ceramide in NPs. Generating gaps (50 scratches/100 mm dish) increased the activity of nSMase by 33+/−10% as quantified by the fluorimetric Amplex red assay (Fig. 3A). Generating half the number of scratches was concurrent with a reduction of nSMase activation by 30%, indicating that nSMase activation was directly correlated with the cell surface area exposed by the scratches.

Immunocytochemistry was performed to detect ceramide and SM at the cell membrane. SM was detected using lysenin, an earth worm protein that binds to SM microdomains, which can then be visualized with an anti-lysenin antibody (Yamaji et al. 1998; Hullin-Matsuda and Kobayashi 2007; Shogomori and Kobayashi 2007). Ceramide was detected using the anti-ceramide rabbit IgG generated in our laboratory (Krishnamurthy et al. 2007a; Krishnamurthy et al. 2007b) and mouse anti-ceramide IgM MAS0020 (Vielhaber et al. 2001; Cowart et al. 2002). Fig. 3B shows that, consistent with activation of nSMase, one hour after wounding of the NP monolayer, ceramide was elevated at the edges of the gaps. In migrating cells, the leading edge and cellular processes stained for ceramide (Fig. 3C). Some membrane areas showed fluorescence signals for both ceramide and SM suggesting that these were sites at which SM was enzymatically converted to ceramide. Migration and process formation was prevented when NPs were incubated with GW4869 (20 μM), an inhibitor of nSMase (Marchesini et al. 2003). Taken together, these results were consistent with activation of nSMase at the migration front and suggested that SM is converted to ceramide in migrating NPs.

In previous studies, we have shown that ceramide binds directly to aPKC and activates the enzyme (Bieberich et al. 2000; Wang et al. 2005; Krishnamurthy et al. 2007b). Consistently, inhibition of aPKC with the myristoylated pseudosubstrate inhibitor of PKCζ/λ (PZI, 15 μM) or the pharmacologic inhibitor Go6983 (1 μM) reduced NP motility by 95% or 73%, respectively. Motility was not affected by inhibition of PKCα, PKCμ, or PKCδ with Go6976 (1 μM) or the respective myristoylated pseudosubstrate inhibitors (15 μM). There was also no reduction of the migration speed by the inhibition of mitogen-activated protein kinase kinase (MEK1) with U0126 (10 μM) or Rho kinase with Y27632 (10 μM). Previous studies have shown the significance of phosphatidylinositols, in particular PIP2 and PIP3 for aPKC-dependent cell polarity (Martin-Belmonte et al. 2007). However, we found that in NPs, inhibition of PIP2 and PIP3 biosynthesis with wortmannin or LY294002 reduced the motility of NPs by less than 30%. Taken together, these results suggested that NP motility was regulated by the effect of ceramide on aPKC.

In processes and membrane protrusions, ceramide was co-distributed with aPKC, Cdc42, α-tubulin, and β-catenin, proteins that are essential for cell motility and adhesion (Figs. 3D and 4A (control), Supplemental Fig. 4) (Etienne-Manneville and Hall 2003b). Ectopic expression of PKCζ-GFP resulted in the formation of processes that were 3-5-fold longer

than with GFP expressing NPs (Supplemental Fig. 5A). The close association of ceramide, aPKC, and α-tubulin in these processes was confirmed by fluorescence resonance energy transfer (FRET) from Cy3 (α-tubulin) to Cy5 (ceramide), which was co-distributed with PKCζ-GFP (Supplemental Fig. 5B). Process formation was abolished when cells were treated with the anti-ceramide antibody.

Incubation with myriocin or treatment with the anti-ceramide antibody also abolished membrane translocation of Cdc42 and co-distribution with aPKC and β-catenin (Fig. 4A, antibody treatment not shown). The effect of myriocin on the membrane translocation of aPKC, and Cdc42 was confirmed using a subcellular fractionation assay. Fig. 4B shows that myriocin treatment reduced the distribution of these two proteins to the membrane fraction. There appeared to be a reduction in the total amount of cytosolic and membrane-associated aPKC, which could be explained by a portion of the protein re-distributing to the nucleus. We then tested if myriocin also prevented the association of aPKC and Cdc42. Using an antibody against aPKC to perform an immunoprecipitation reaction, Cdc42 was no longer co-immunoprecipitated with aPKC when cells were depleted of ceramide (Fig. 4C). The upper panel shows the loading control confirming that equal amounts of cellular protein were used for the co-immunoprecipitation reaction with untreated or myriocin-treated NPs. This result was consistent with that of a similar assay previously performed with primitive ectoderm cells, indicating that ceramide was critical for the membrane translocation and interaction of aPKC with Cdc42 in various embryonic cell types (Krishnamurthy et al. 2007b).

Since inactivation of GSK-3β stabilizes β-catenin (Etienne-Manneville and Hall 2003b), we tested whether diminished membrane translocation of aPKC affected the level of GSK-3β phosphorylation and the protein level of β-catenin. Fig. 4D shows that in myriocin-treated NPs, the phosphorylation of GSK-3β at serine 9 and the β-catenin level were concomitantly down-regulated. To evaluate the significance of GSK-3β inactivation on NP motility, we performed scratch migration assays in the presence of lithium chloride (LiCl), a GSK-3β inhibitor (van Noort et al. 2002). Supplementation of LiCl to the myriocin-treated cells partially restored the number of migrating cells (Fig. 1C), indicating that myriocin reduced cell motility via aberrant activation of GSK-3β. In summary, these results suggest that the ceramide-mediated membrane translocation/association of aPKC and Cdc42 inhibits GSK-3β and may stabilize β-catenin and microtubules, which is both required for NP polarity and motility.

Sphingolipid depletion perturbs the distribution of mitotic and post-mitotic cells in NP rosettes and in embryos

From the phenotypes of conditional, NP-specific knockout mice for aPKC and its associated proteins Cdc42 and β-catenin it is known that these proteins are critical for the organization of the embryonic brain neuroepithelium (Chen et al. 2006; Imai et al. 2006). The effect of myriocin treatment on membrane translocation of these proteins suggested that sphingolipids are important for the regulation of aPKC and its associated proteins during brain development. This hypothesis was tested in two model systems for embryonic brain development: *in vitro* differentiated ES cells and mouse embryos *in vivo*. ES cell-derived NPs were differentiated to post-mitotic, early neurons that showed a distinct distribution in so-called rosette structures (Fig. 4E and F) (Lazzari et al. 2006). Post-mitotic (β-tubulin III or Tuj1(+)) neurons were in the periphery, while mitotic cells in G2/M-phase (phospho-histone 3 or pH3(+)) were localized in the center of the NP rosette (arrows in Fig. 4E). This distribution of mitotic and post-mitotic cells was typical for NPs when cultivated for 48-96 h in differentiation medium (withdrawal of FGF-2). The polarized distribution was completely abolished when NPs were treated with myriocin 48 h before transferring cells to differentiation medium (Fig. 4F). However, it should be noted that only the polarized

distribution, but not the formation of mitotic (pH3(+)) or post-mitotic (Tuj1(+)) cells was affected.

Rosettes consisting of mitotic NPs and post-mitotic neuronal precursors have been suggested to recapitulate the polarized distribution of NPs in the neuroepithelium with the center of the rosette representing dividing cells at the apical, ventricular surface (Lazzari et al. 2006). We reasoned that our experimental strategy to deplete NPs of sphingolipids *in vitro* may be applicable to embryos *in vivo.* We administered myriocin to pregnant mice by intraperitoneal (i.p.) injection of 1 mg/kg body weight every 48 h from gestational day E11.5 to E16.5. We found that this dose was well tolerated, not causing maternal or embryonic lethality or other signs of toxicity. The quantitative lipid analysis in Fig. 5A shows that consistent with results from *in vitro* differentiated NPs, overall ceramide levels in myriocin-treated embryos were reduced by more than 50% (from 2.0+/−0.3 to 0.8+/−0.2 μg/mg cell protein, lanes 4 and 5). Also consistent with the results obtained from *in vitro* differentiated NPs, myriocin treatment reduced the phosphorylation of GSK-3β and the protein level of β-catenin in embryos (Figs. 4D and 5B).

Immunohistochemistry showed that the apical membrane of NPs in the neuroepithelium of E16.5 mouse brain was enriched with ceramide, which was co-distributed with aPKC and β-catenin (Fig. 5C). This co-distribution was consistent with that found for ES cell-derived NPs (Fig. 4A (control)). Myriocin treatment of embryos *in utero* reduced the overall fluorescence signal for ceramide (Fig. 5D). This result clearly demonstrated the validity of myriocin treatment to deplete embryos of sphingolipids and confirmed the specificity of the antibody reaction. In particular, myriocin treatment abolished the fluorescence signal for ceramide in the apical membrane and obliterated the apical co-distribution of aPKC and β-catenin (Fig. 5D).

Most intriguingly, loss of ceramide in the apical membrane of the periventricular neuroepithelium resulted in dramatic changes of embryonic brain organization. In the neuroepithelium of control brains, periventricular cells were pseudo-stratified/elongated with their nuclei aligned perpendicular to the ventricular surface (Topro-3-stained in Fig. 6A, left panel). Immunocytochemistry showed that this alignment correlated with the distribution of β-catenin in the apical and lateral cell membranes (arrows in Fig. 6A, left panel). Tuj1 was mostly absent from the neuroepithelium (Fig. 6A, left panel). In myriocin-treated embryos, the expression of β-catenin in the neuroepithelium was dramatically reduced and the ordered alignment of nuclei was obliterated. Instead, cells were rounded up and their nuclei were randomly distributed (Fig. 6A, right panel).

Fig. 6B confirms that myriocin treatment *in utero* resulted in the ectopic localization of Tuj1(+) neuronal precursors, which was consistent with the result found with NP rosettes (Fig. 4F). In fact, the border of the intermediate zone/cortical plate (IZ/CP) cell layers was no longer detectable. Most strikingly, S18 restored the normal distribution of neuronal precursors, without replenishing apical ceramide (Fig. 6B, right panel). This result was consistent with that obtained with *in vitro* differentiated NPs and suggested that S18 functionally replaced missing ceramide in neuroepithelial cells. Consistent with the *in vitro* results was also the ectopic distribution of mitotic (pH3(+)) NPs (Fig. 7A and B) to the intermediate zone, which was absent in control embryos (Fig. 7A and B). S18 restored the wild-type distribution of mitotic cells (Fig. 7B), which further supports the significance of ceramide for the normal organization of the embryonic brain. It should be noted that the total number of mitotic cells was similar for control, myriocin, and myriocin/S18-treated embryos. This was consistent with the results obtained with ES cell-derived NP rosettes (Fig. 4E and F) suggesting that ceramide is critical for the apico-basal distribution and/or attachment of mitotic NPs in the neuroepithelium.

We then tested the effect of intermittent sphingolipid depletion *in utero* on newborn pups. Pregnant mice were administered with myriocin from day E11.5-E15.5, followed by myriocin-free recovery until the time point of delivery. Pups were born alive, but they did not survive the first day. The brain of the newborns was analyzed using immunocytochemistry for neuronal markers. Supplemental Fig. 6 shows that myriocin treatment between day E11.5 and E15.5 resulted in thickening of the cortex and dramatic changes of the distribution of the neuronal marker protein Map-2. The border between the intermediate zone and the cortical layer disappeared consistent with the results obtained from E16.5 brains (Fig. 6B, middle panel). Taken together, these results suggest that ceramide critically regulates the distribution of cells in the proliferative neuroepithelium and is required for normal embryonic brain organization.

DISCUSSION

The membrane translocation and activation of aPKC is critical for the regulation of adhesion, polarity, and migration in neural cells (Etienne-Manneville and Hall 2003b; Cau and Hall 2005; Imai et al. 2006). In these processes, a re-occurring protein complex of aPKC with Par6, Par3, Cdc42, GSK-3β, and β-catenin translates the membrane translocation and activation of aPKC into the regulation of cytoskeletal dynamics and cell motility (Etienne-Manneville and Hall 2003b; Solecki et al. 2004). However, little is known about how aPKC itself is initially activated at specific sub-cellular locations. Previous studies in our and other laboratories have shown that ceramide activates aPKC and recruits the enzyme to the cell membrane (Wang et al. 2005; Fox et al. 2007; Krishnamurthy et al. 2007b). Our goal in this study was to determine the significance of the ceramide-dependent regulation of aPKC for NP motility and embryonic brain development.

We decided to use incubation with different ceramide species/analogs and pharmacologic inhibitors of *de novo* sphingolipid biosynthesis to enhance or reduce the level of ceramide or sphingolipids in NPs and embryonic mouse brain. The two inhibitors, myriocin and FB1 have been shown to be specific for serine palmitoyltransferase and (dihydro)ceramide synthase, respectively (Chalfant et al. 2002; Desai et al. 2002; He et al. 2004). Due to their lipophilic character they are able to cross various endothelial blood-tissue barriers allowing their effective use as drugs *in vivo* (Johnson et al. 2004; Marasas et al. 2004; Gelineau-van Waes et al. 2005). The advantage of using specific pharmacologic inhibitors is their immediate effect on blocking ceramide biosynthesis without first depriving cells of the respective enzyme. The disadvantage of pharmacologic as well as any other approaches blocking the expression of biosynthetic enzymes is that they not only reduce the level of ceramide, but also that of its derivatives (Riley et al. 1999; Krishnamurthy et al. 2007b).

In this study, two independent observations suggest that ceramide is the key factor regulating aPKC-dependent processes such as cell polarity and motility: The first line of evidence comes from the ability of particular ceramide species or analogs to enhance motility and to rescue the phenotype of sphingolipid-depleted cells and embryos. Incubation with C16 ceramide, C18:1 ceramide, or endogenous ceramide restores the motility and subcellular distribution of aPKC and its associated proteins in myriocin- or anti-ceramide antibody-treated NPs. The motility of NPs is also enhanced or restored with the water-soluble ceramide analog N-oleoyl serinol (S18) suggesting that it is a functional mimic of ceramide. This assumption is consistent with the observation that S18 rescues the brain phenotype in myriocin-treated embryos. The effect of ceramide appears to be specific for distinct ceramide types since the two other water-soluble analogs of ceramide, C2 or C8 ceramide do not restore NP motility. Accordingly, these analogs were precluded from their use *in vivo*. The failure of C8 ceramide to rescue motility in myriocin-treated NPs is interesting in that it is consistent with the result of a previous study showing that C6

ceramide did not restore process formation in FB1-treated 3T3 fibroblasts (Meivar-Levy et al. 1997). In other cell types, it has been shown that short chain ceramide, in particular C6 ceramide, is taken up by endocytosis and converted to endogenous (long chain) ceramide via the salvage pathway (Ogretmen et al. 2002). Our results, however, suggest that C2 and C8 ceramide are poor substrates for this pathway in NPs, which is consistent with previous studies (Ogretmen et al. 2002). The inability of C2 and C8 ceramide to restore migration in myriocin-treated NPs is also consistent with the assumption that scratch-induced migration relies on the release of ceramide from SM, which requires additional biosynthetic and transport steps if SM is first generated by the salvage pathway.

The second line of evidence for a specific effect of ceramide comes from the failure of sphingolipids other than ceramide to restore motility in myriocin-treated NPs. Inhibition of glycolipid biosynthesis with N-butyl deoxinojirimycin (Bieberich et al. 2001; Krishnamurthy et al. 2007a) did not prevent process formation or reduce NP motility. This observation is consistent with the phenotypes of various conventional and conditional knockout mice for glycolipids indicating that this lipid class is not required for the aPKC-dependent regulation of cell adhesion or motility (Yamashita et al. 2005a; Yamashita et al. 2005b). However, our results do not rule out the critical involvement of glycolipids in other aspects of brain development. A similar conclusion is drawn for S1P, which did not restore motility in myriocin-treated NPs. S1P has been shown to act as a chemoattractant in rat brain-derived NPs (Kimura et al. 2007). Therefore, S1P may not increase cell motility, but may be a chemoattractant that induces chemotaxis toward an S1P gradient. The S1P-dependent cell signaling pathway inducing chemotaxis is likely to be different from that for ceramide-dependent cell motility. Sphingomyelin (SM), however, appears to be involved in ceramide-dependent motility. This conclusion is supported by the observation that wounding of the NP monolayer activates nSMase and elevates ceramide in cells at the edges of the wounding gaps. It is also consistent with the effect of the nSMase inhibitor GW4869 to prevent scratch-induced migration. Based on these results, we conclude that SM serves as metabolic precursor, the hydrolysis of which may be activated by mechanical stress and may initiate the ceramide-dependent regulation of NP motility.

The phenotype of the NP-specific conditional knockout mouse for aPKC clearly demonstrates that aPKC is essential for cell polarity, adhesion, and migration of NPs (Imai et al. 2006). This phenotype is consistent with results of the scratch migration assay showing that inhibition of aPKC with the myristoylated pseudosubstrate inhibitor of PKCζ/λ (PZI) or Go6983 obliterates cell motility. The phenotype of the NP-specific aPKC knockout mouse and the effect of the aPKC inhibitors may not be surprising since many of the immediate downstream targets of aPKC are involved in cell polarity, adhesion, and motility. Among the target proteins that have been suggested or shown to be phosphorylated by aPKC are GSK-3β, Numb, and lethal giant larvae (lgl) (Plant et al. 2003; Lee et al. 2006). Phosphorylation inhibits GSK-3β, which in turn stabilizes β-catenin and microtubules at the apical membrane (Etienne-Manneville and Hall 2003b), while phosphorylation of Numb and lgl induces their distribution to the basal and basolateral membrane of polarized cells (Lee et al. 2006). Atypical PKC-associated protein complexes establishing apico-basal polarity are typical for epithelial cells and they are also involved the front-rear polarity of migrating cells (Etienne-Manneville and Hall 2003b). Phosphorylation and inhibition of GSK-3β in an aPKC-associated protein complex appears to be an important downstream effect of ceramide since LiCl restores motility in myriocin-treated cells. Therefore, activation of aPKC and its associated protein complexes will regulate cell polarity as well as motility. Further, aPKC and β-catenin are critical for cell adhesion of epithelial cells (Manabe et al. 2002), which implies that the activation of aPKC and formation of aPKC-associated protein complex requires a dynamic regulation.

One of the main regulatory factors in polarity complexes is Cdc42, a small GTPase that is associated with aPKC via binding to Par6 (Martin-Belmonte et al. 2007). It has been shown that in MDCK cells, membrane-bound Cdc42 recruits aPKC, which then initiates the formation of a polarity complex (Martin-Belmonte et al. 2007). However, the results of our study suggest that the interaction of aPKC with Cdc42 requires ceramide or a ceramide derivative. This is supported by the experiments using myriocin, which prevents 1) membrane association of aPKC and Cdc42 and 2) interaction of Cdc42 with aPKC. The assumption that it is ceramide that is critical for the interaction of aPKC with Par6 and Cdc42 stems from the observation that C16 ceramide, endogenous ceramide, and S18 enhance or restore membrane co-distribution of aPKC and Cdc42, and motility in myriocin or anti-ceramide antibody-treated NPs. It should also be noted that our previous studies have shown that ceramide-containing lipid vesicles bind to aPKC, Par6, and Cdc42 in an *in vitro* reconstitution assay (Krishnamurthy et al. 2007b). Therefore, it is logical to assume that a similar ceramide-bound protein complex is formed *in vivo*.

Although our results point at ceramide-activated aPKC as key factor regulating cell motility, it is possible that other ceramide-activated proteins participate in the organization of polarity complexes. In addition to aPKC, protein phosphatases 2A (PP2A) and 1 (PP1) are known to be activated by ceramide (Dobrowsky et al. 1993; Chalfant et al. 2004). Remarkably, inhibition of GSK-3β by ceramide-activated aPKC and dephosphorylation of β-catenin by ceramide-activated PP2A or PP1 will have the same outcome (stabilization of β-catenin and microtubules), thereby acting synergistically on cell polarity and motility. This assumption is supported by a recent study showing that ceramide-activated PP1γc de-phosphorylates β-catenin when MCF-7 cells reach confluence (Marchesini et al. 2007). This suggests that ceramide may specifically target aPKC or PP1 in processes related to apico-basal polarity and motility or confluence, respectively. It has been shown that ceramide-mediated activation of PP1 affects alternative splicing of apoptosis-related proteins such as b-cell lymphoma × (bcl-x) or caspase 9 (Chalfant et al. 2002). Although this mechanism may also affect alternative splicing of polarity proteins such as Par3 (Gao et al. 2002), it cannot explain the rapid effect of ceramide or S18 on the increase or restoration of NP motility as determined in scratch migration assays. Therefore, we conclude that the effect of ceramide on cell motility or polarity is rather mediated by rapid processes such as enzyme activation/translocation of aPKC.

This is the first report showing the effect of ceramide on embryonic brain development. It suggests a polarity-organizing function of ceramide that is distinct from its pro-apoptotic effect in other cells. Our data supports the hypothesis that ceramide is a key regulatory factor in embryo brain development and that its effect, inducing apoptosis or sustaining cell polarity depends on the ceramide-induced association of specific proteins with aPKC.

Supplementary Material

Refer to Web version on PubMed Central for supplementary material.

Acknowledgments

The authors are indebted to Mrs. Arti Jain for her technical assistance. We thank the Imaging Core Facility under supervision of Drs. Paul McNeil and Katsuya Miyake (Medical College of Georgia, Augusta, GA) for their technical assistance. We also thank Mrs. LaTricia Faison (Histopathology Core facility under the supervision of Dr. Jeffrey Lee, Medical College of Georgia) for assistance with the cryosections. We thank Dr. Robert K. Yu for institutional support. This work was funded by NIH grant R01NS046835.

ABBREVIATIONS

aPKC	atypical PKCζ/λ
C16 ceramide	C16:0 ceramide or N-palmitoyl D-erythro sphingosine
C2 ceramide	N-acetoyl D-erythro sphingosine
C8 ceramide	N-octanoyl D-erythro sphingosine
C18:1 ceramide	N-oleoyl D-erythro sphingosine
NPs	neural progenitor cells
GSK-3β	glycogen synthase kinase 3β
FB1	fumonisin B1
Myr	myriocin
pH3	phospho-histone 3
PIPs	phosphoinositolphosphates
S18	N-oleoyl serinol
SM	sphingomyelin
nSMase	neutral sphingomyelinase
S1P	sphingosine 1 phosphate
SPT	serine palmitoyltransferase
Tuj1	β tubulin III

REFERENCES

Bieberich E, Kawaguchi T, Yu RK. N-acylated serinol is a novel ceramide mimic inducing apoptosis in neuroblastoma cells. The Journal of biological chemistry. 2000; 275:177–181. [PubMed: 10617602]

Bieberich E, MacKinnon S, Silva J, Yu RK. Regulation of apoptosis during neuronal differentiation by ceramide and b-series complex gangliosides. The Journal of biological chemistry. 2001; 276:44396–44404. [PubMed: 11574545]

Bieberich E, MacKinnon S, Silva J, Noggle S, Condie BG. Regulation of cell death in mitotic neural progenitor cells by asymmetric distribution of prostate apoptosis response 4 (PAR-4) and simultaneous elevation of endogenous ceramide. J Cell Biol. 2003; 162:469–479. [PubMed: 12885759]

Bieberich E, Silva J, Wang G, Krishnamurthy K, Condie BG. Selective apoptosis of pluripotent mouse and human stem cells by novel ceramide analogues prevents teratoma formation and enriches for neural precursors in ES cell-derived neural transplants. J Cell Biol. 2004; 167:723–734. [PubMed: 15545317]

Bieberich E, Hu B, Silva J, MacKinnon S, Yu RK, Fillmore H, Broaddus WC, Ottenbrite RM. Synthesis and characterization of novel ceramide analogs for induction of apoptosis in human cancer cells. Cancer Lett. 2002; 181:55–64. [PubMed: 12430179]

Bourbon NA, Yun J, Kester M. Ceramide directly activates protein kinase C zeta to regulate a stress-activated protein kinase signaling complex. The Journal of biological chemistry. 2000; 275:35617–35623. [PubMed: 10962008]

Cappello S, Attardo A, Wu X, Iwasato T, Itohara S, Wilsch-Brauninger M, Eilken HM, Rieger MA, Schroeder TT, Huttner WB, Brakebusch C, Gotz M. The Rho-GTPase cdc42 regulates neural progenitor fate at the apical surface. Nat Neurosci. 2006; 9:1099–1107. [PubMed: 16892058]

Cau J, Hall A. Cdc42 controls the polarity of the actin and microtubule cytoskeletons through two distinct signal transduction pathways. J Cell Sci. 2005; 118:2579–2587. [PubMed: 15928049]

Chalfant CE, Szulc Z, Roddy P, Bielawska A, Hannun YA. The structural requirements for ceramide activation of serine-threonine protein phosphatases. J Lipid Res. 2004; 45:496–506. [PubMed: 14657198]

Chalfant CE, Rathman K, Pinkerman RL, Wood RE, Obeid LM, Ogretmen B, Hannun YA. De novo ceramide regulates the alternative splicing of caspase 9 and Bcl-x in A549 lung adenocarcinoma cells. Dependence on protein phosphatase-1. The Journal of biological chemistry. 2002; 277:12587–12595. [PubMed: 11801602]

Chen L, Liao G, Yang L, Campbell K, Nakafuku M, Kuan CY, Zheng Y. Cdc42 deficiency causes Sonic hedgehog-independent holoprosencephaly. Proc Natl Acad Sci U S A. 2006; 103:16520–16525. [PubMed: 17050694]

Clarke CJ, Hannun YA. Neutral sphingomyelinases and nSMase2: bridging the gaps. Biochim Biophys Acta. 2006; 1758:1893–1901. [PubMed: 16938269]

Clarke CJ, Snook CF, Tani M, Matmati N, Marchesini N, Hannun YA. The extended family of neutral sphingomyelinases. Biochemistry. 2006; 45:11247–11256. [PubMed: 16981685]

Cowart LA, Szulc Z, Bielawska A, Hannun YA. Structural determinants of sphingolipid recognition by commercially available anti-ceramide antibodies. J Lipid Res. 2002; 43:2042–2048. [PubMed: 12454264]

Dasgupta S, Hogan EL. Chromatographic resolution and quantitative assay of CNS tissue sphingoids and sphingolipids. J Lipid Res. 2001; 42:301–308. [PubMed: 11181761]

Desai K, Sullards MC, Allegood J, Wang E, Schmelz EM, Hartl M, Humpf HU, Liotta DC, Peng Q, Merrill AH Jr. Fumonisins and fumonisin analogs as inhibitors of ceramide synthase and inducers of apoptosis. Biochim Biophys Acta. 2002; 1585:188–192. [PubMed: 12531553]

Dobrowsky RT, Kamibayashi C, Mumby MC, Hannun YA. Ceramide activates heterotrimeric protein phosphatase 2A. The Journal of biological chemistry. 1993; 268:15523–15530. [PubMed: 8393446]

Etienne-Manneville S, Hall A. Integrin-mediated activation of Cdc42 controls cell polarity in migrating astrocytes through PKCzeta. Cell. 2001; 106:489–498. [PubMed: 11525734]

Etienne-Manneville S, Hall A. Rho GTPases in cell biology. Nature. 2002; 420:629–635. [PubMed: 12478284]

Etienne-Manneville S, Hall A. Cell polarity: Par6, aPKC and cytoskeletal crosstalk. Curr Opin Cell Biol. 2003a; 15:67–72. [PubMed: 12517706]

Etienne-Manneville S, Hall A. Cdc42 regulates GSK-3beta and adenomatous polyposis coli to control cell polarity. Nature. 2003b; 421:753–756. [PubMed: 12610628]

Fox TE, Houck KL, O'Neill SM, Nagarajan M, Stover TC, Pomianowski PT, Unal O, Yun JK, Naides SJ, Kester M. Ceramide recruits and activates PKCzeta within structured membrane microdomains. The Journal of biological chemistry. 2007

Gao L, Macara IG, Joberty G. Multiple splice variants of Par3 and of a novel related gene, Par3L, produce proteins with different binding properties. Gene. 2002; 294:99–107. [PubMed: 12234671]

Gelineau-van Waes J, Starr L, Maddox J, Aleman F, Voss KA, Wilberding J, Riley RT. Maternal fumonisin exposure and risk for neural tube defects: mechanisms in an in vivo mouse model. Birth Defects Res A Clin Mol Teratol. 2005; 73:487–497. [PubMed: 15959874]

Hajduch E, Turban S, Le Liepvre X, Le Lay S, Lipina C, Dimopoulos N, Dugail I, Hundal HS. Targeting of PKCzeta and PKB to caveolin-enriched microdomains represents a crucial step underpinning the disruption in PKB-directed signaling by ceramide. Biochem J. 2007

Hatten ME. Central nervous system neuronal migration. Annu Rev Neurosci. 1999; 22:511–539. [PubMed: 10202547]

He Q, Johnson VJ, Osuchowski MF, Sharma RP. Inhibition of serine palmitoyltransferase by myriocin, a natural mycotoxin, causes induction of c-myc in mouse liver. Mycopathologia. 2004; 157:339–347. [PubMed: 15180163]

Horne-Badovinac S, Lin D, Waldron S, Schwarz M, Mbamalu G, Pawson T, Jan Y, Stainier DY, Abdelilah-Seyfried S. Positional cloning of heart and soul reveals multiple roles for PKC lambda in zebrafish organogenesis. Curr Biol. 2001; 11:1492–1502. [PubMed: 11591316]

Hullin-Matsuda F, Kobayashi T. Monitoring the distribution and dynamics of signaling microdomains in living cells with lipid-specific probes. Cell Mol Life Sci. 2007

Imai F, Hirai S, Akimoto K, Koyama H, Miyata T, Ogawa M, Noguchi S, Sasaoka T, Noda T, Ohno S. Inactivation of aPKClambda results in the loss of adherens junctions in neuroepithelial cells without affecting neurogenesis in mouse neocortex. Development. 2006; 133:1735–1744. [PubMed: 16571631]

Johnson VJ, He Q, Osuchowski MF, Sharma RP. Disruption of sphingolipid homeostasis by myriocin, a mycotoxin, reduces thymic and splenic T-lymphocyte populations. Toxicology. 2004; 201:67–75. [PubMed: 15297021]

Kay AJ, Hunter CP. CDC-42 regulates PAR protein localization and function to control cellular and embryonic polarity in C. elegans. Curr Biol. 2001; 11:474–481. [PubMed: 11412996]

Kimura A, Ohmori T, Ohkawa R, Madoiwa S, Mimuro J, Murakami T, Kobayashi E, Hoshino Y, Yatomi Y, Sakata Y. Essential roles of sphingosine 1-phosphate/S1P1 receptor axis in the migration of neural stem cells toward a site of spinal cord injury. Stem cells (Dayton, Ohio). 2007; 25:115–124.

Kitchens DL, Snyder EY, Gottlieb DI. FGF and EGF are mitogens for immortalized neural progenitors. J Neurobiol. 1994; 25:797–807. [PubMed: 8089657]

Koike C, Nishida A, Akimoto K, Nakaya MA, Noda T, Ohno S, Furukawa T. Function of atypical protein kinase C lambda in differentiating photoreceptors is required for proper lamination of mouse retina. J Neurosci. 2005; 25:10290–10298. [PubMed: 16267237]

Krishnamurthy K, Dasgupta S, Bieberich E. Development and characterization of a novel anti-ceramide antibody. J Lipid Res. 2007a

Krishnamurthy K, Wang G, Silva J, Condie BG, Bieberich E. Ceramide Regulates Atypical PKC{zeta}/{lambda}-mediated Cell Polarity in Primitive Ectoderm Cells: A NOVEL FUNCTION OF SPHINGOLIPIDS IN MORPHOGENESIS. The Journal of biological chemistry. 2007b; 282:3379–3390. [PubMed: 17105725]

Lazzari G, Colleoni S, Giannelli SG, Brunetti D, Colombo E, Lagutina I, Galli C, Broccoli V. Direct derivation of neural rosettes from cloned bovine blastocysts: a model of early neurulation events and neural crest specification in vitro. Stem cells (Dayton, Ohio). 2006; 24:2514–2521.

Lee CY, Robinson KJ, Doe CQ. Lgl, Pins and aPKC regulate neuroblast self-renewal versus differentiation. Nature. 2006; 439:594–598. [PubMed: 16357871]

Liu XF, Ohno S, Miki T. Nucleotide exchange factor ECT2 regulates epithelial cell polarity. Cell Signal. 2006; 18:1604–1615. [PubMed: 16495035]

Liu XF, Ishida H, Raziuddin R, Miki T. Nucleotide exchange factor ECT2 interacts with the polarity protein complex Par6/Par3/protein kinase Czeta (PKCzeta) and regulates PKCzeta activity. Mol Cell Biol. 2004; 24:6665–6675. [PubMed: 15254234]

Lopez-Montero I, Rodriguez N, Cribier S, Pohl A, Velez M, Devaux PF. Rapid transbilayer movement of ceramides in phospholipid vesicles and in human erythrocytes. J Biol Chem. 2005; 280:25811–25819. [PubMed: 15883154]

Lozano J, Berra E, Municio MM, Diaz-Meco MT, Dominguez I, Sanz L, Moscat J. Protein kinase C zeta isoform is critical for kappa B-dependent promoter activation by sphingomyelinase. The Journal of biological chemistry. 1994; 269:19200–19202. [PubMed: 8034680]

Machon O, van den Bout CJ, Backman M, Kemler R, Krauss S. Role of beta-catenin in the developing cortical and hippocampal neuroepithelium. Neuroscience. 2003; 122:129–143. [PubMed: 14596855]

Manabe N, Hirai S, Imai F, Nakanishi H, Takai Y, Ohno S. Association of ASIP/mPAR-3 with adherens junctions of mouse neuroepithelial cells. Dev Dyn. 2002; 225:61–69. [PubMed: 12203721]

Marasas WF, Riley RT, Hendricks KA, Stevens VL, Sadler TW, Gelineau-van Waes J, Missmer SA, Cabrera J, Torres O, Gelderblom WC, Allegood J, Martinez C, Maddox J, Miller JD, Starr L, Sullards MC, Roman AV, Voss KA, Wang E, Merrill AH Jr. Fumonisins disrupt sphingolipid metabolism, folate transport, and neural tube development in embryo culture and in vivo: a potential risk factor for human neural tube defects among populations consuming fumonisin-contaminated maize. J Nutr. 2004; 134:711–716. [PubMed: 15051815]

Marchesini N, Luberto C, Hannun YA. Biochemical properties of mammalian neutral sphingomyelinase 2 and its role in sphingolipid metabolism. The Journal of biological chemistry. 2003; 278:13775–13783. [PubMed: 12566438]

Marchesini N, Jones JA, Hannun YA. Confluence induced threonine41/serine45 phospho-beta-catenin dephosphorylation via ceramide-mediated activation of PP1cgamma. Biochim Biophys Acta. 2007

Marin O, Rubenstein JL. Cell migration in the forebrain. Annu Rev Neurosci. 2003; 26:441–483. [PubMed: 12626695]

Martin-Belmonte F, Gassama A, Datta A, Yu W, Rescher U, Gerke V, Mostov K. PTEN-mediated apical segregation of phosphoinositides controls epithelial morphogenesis through Cdc42. Cell. 2007; 128:383–397. [PubMed: 17254974]

Meivar-Levy I, Sabanay H, Bershadsky AD, Futerman AH. The role of sphingolipids in the maintenance of fibroblast morphology. The inhibition of protrusional activity, cell spreading, and cytokinesis induced by fumonisin B1 can be reversed by ganglioside GM3. The Journal of biological chemistry. 1997; 272:1558–1564. [PubMed: 8999828]

Muller G, Ayoub M, Storz P, Rennecke J, Fabbro D, Pfizenmaier K. PKC zeta is a molecular switch in signal transduction of TNF-alpha, bifunctionally regulated by ceramide and arachidonic acid. Embo J. 1995; 14:1961–1969. [PubMed: 7744003]

Ogretmen B, Pettus BJ, Rossi MJ, Wood R, Usta J, Szulc Z, Bielawska A, Obeid LM, Hannun YA. Biochemical mechanisms of the generation of endogenous long chain ceramide in response to exogenous short chain ceramide in the A549 human lung adenocarcinoma cell line. Role for endogenous ceramide in mediating the action of exogenous ceramide. The Journal of biological chemistry. 2002; 277:12960–12969. [PubMed: 11815611]

Ohno S. Intercellular junctions and cellular polarity: the PAR-aPKC complex, a conserved core cassette playing fundamental roles in cell polarity. Curr Opin Cell Biol. 2001; 13:641–648. [PubMed: 11544035]

Plant PJ, Fawcett JP, Lin DC, Holdorf AD, Binns K, Kulkarni S, Pawson T. A polarity complex of mPar-6 and atypical PKC binds, phosphorylates and regulates mammalian Lgl. Nat Cell Biol. 2003; 5:301–308. [PubMed: 12629547]

Riess P, Zhang C, Saatman KE, Laurer HL, Longhi LG, Raghupathi R, Lenzlinger PM, Lifshitz J, Boockvar J, Neugebauer E, Snyder EY, McIntosh TK. Transplanted neural stem cells survive, differentiate, and improve neurological motor function after experimental traumatic brain injury. Neurosurgery. 2002; 51:1043–1052. discussion 1052-1044. [PubMed: 12234415]

Riley RT, Norred WP, Wang E, Merrill AH. Alteration in sphingolipid metabolism: bioassays for fumonisin- and ISP-I-like activity in tissues, cells and other matrices. Nat Toxins. 1999; 7:407–414. [PubMed: 11122537]

Shogomori H, Kobayashi T. Lysenin: A sphingomyelin specific pore-forming toxin. Biochim Biophys Acta. 2007

Solecki DJ, Model L, Gaetz J, Kapoor TM, Hatten ME. Par6alpha signaling controls glial-guided neuronal migration. Nat Neurosci. 2004; 7:1195–1203. [PubMed: 15475953]

Soloff RS, Katayama C, Lin MY, Feramisco JR, Hedrick SM. Targeted deletion of protein kinase C lambda reveals a distribution of functions between the two atypical protein kinase C isoforms. J Immunol. 2004; 173:3250–3260. [PubMed: 15322187]

van Noort M, Meeldijk J, van der Zee R, Destree O, Clevers H. Wnt signaling controls the phosphorylation status of beta-catenin. The Journal of biological chemistry. 2002; 277:17901–17905. [PubMed: 11834740]

Vielhaber G, Brade L, Lindner B, Pfeiffer S, Wepf R, Hintze U, Wittern KP, Brade H. Mouse anti-ceramide antiserum: a specific tool for the detection of endogenous ceramide. Glycobiology. 2001; 11:451–457. [PubMed: 11445550]

Wang G, Silva J, Krishnamurthy K, Tran E, Condie BG, Bieberich E. Direct binding to ceramide activates protein kinase Czeta before the formation of a pro-apoptotic complex with PAR-4 in differentiating stem cells. The Journal of biological chemistry. 2005; 280:26415–26424. [PubMed: 15901738]

Wang YM, Seibenhener ML, Vandenplas ML, Wooten MW. Atypical PKC zeta is activated by ceramide, resulting in coactivation of NF-kappaB/JNK kinase and cell survival. J Neurosci Res. 1999; 55:293–302. [PubMed: 10348660]

Welchman DP, Mathies LD, Ahringer J. Similar requirements for CDC-42 and the PAR-3/PAR-6/PKC-3 complex in diverse cell types. Dev Biol. 2007; 305:347–357. [PubMed: 17383625]

Wessel D, Flugge UI. A method for the quantitative recovery of protein in dilute solution in the presence of detergents and lipids. Anal Biochem. 1984; 138:141–143. [PubMed: 6731838]

Yamaji A, Sekizawa Y, Emoto K, Sakuraba H, Inoue K, Kobayashi H, Umeda M. Lysenin, a novel sphingomyelin-specific binding protein. The Journal of biological chemistry. 1998; 273:5300–5306. [PubMed: 9478988]

Yamashita T, Allende ML, Kalkofen DN, Werth N, Sandhoff K, Proia RL. Conditional LoxP-flanked glucosylceramide synthase allele controlling glycosphingolipid synthesis. Genesis. 2005a; 43:175–180. [PubMed: 16283624]

Yamashita T, Wu YP, Sandhoff R, Werth N, Mizukami H, Ellis JM, Dupree JL, Geyer R, Sandhoff K, Proia RL. Interruption of ganglioside synthesis produces central nervous system degeneration and altered axon-glial interactions. Proc Natl Acad Sci U S A. 2005b; 102:2725–2730. [PubMed: 15710896]

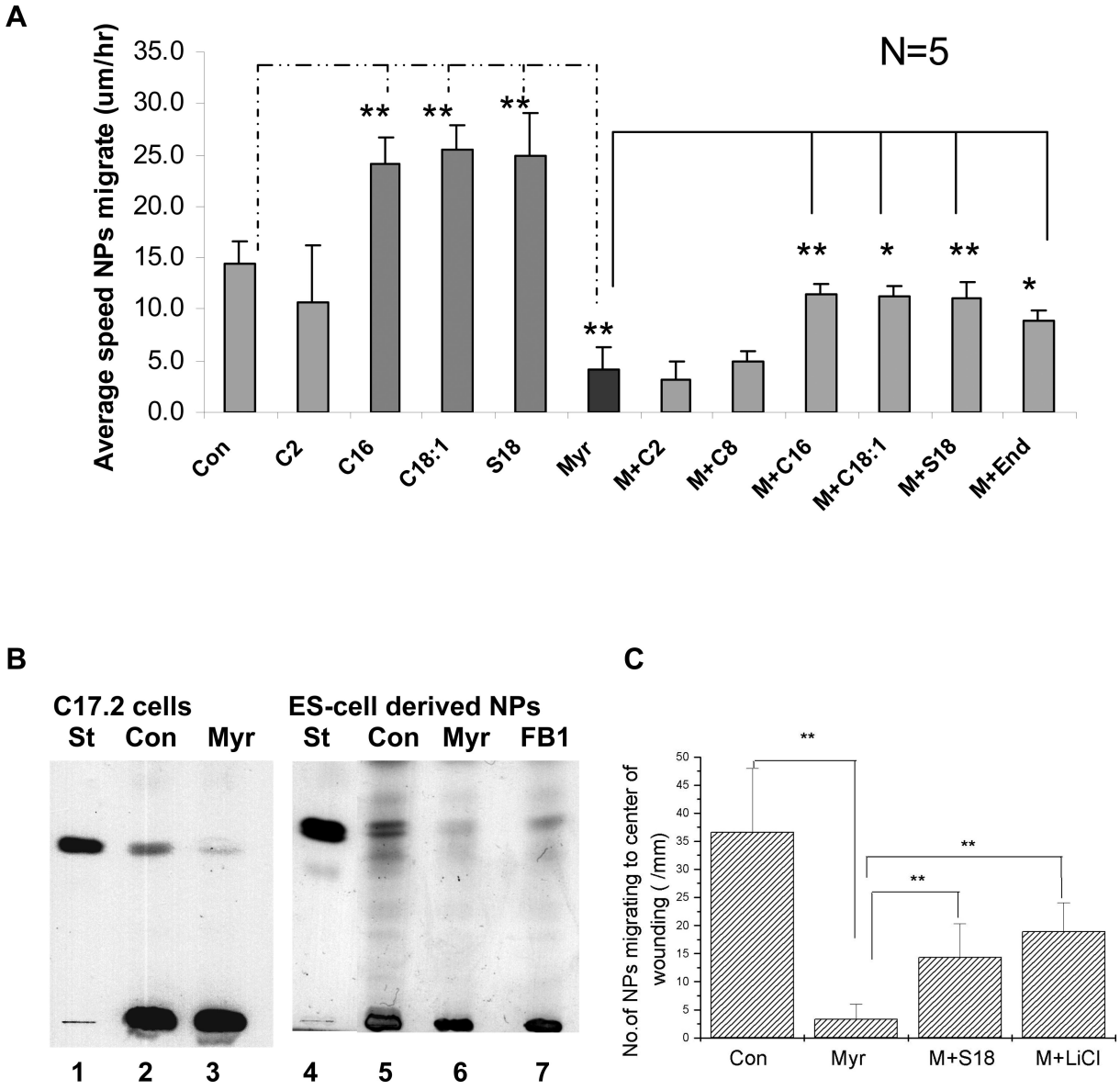

Fig. 1. Ceramide and S18 enhance migration, while sphingolipid depletion prevents motility of C17.2 cells and ES cell-derived NPs

A. Various ceramide species or S18 was added one hour before generating the gap in a scratch migration assay. The average speed of migration of C17.2 cells was determined within 2-6 h after generating the gap. M, myr, Myriocin; C2, C2 ceramide; C8, C8 ceramide; C16, C16 ceramide; C18:1, C18:1 ceramide; End, endogenous ceramide; S18, N-oleoyl serinol. **B**. HPTLC analysis of lipids extracted after incubation of C17.2 cells (left panel) or ES cell-derived NPs (right panel) with myriocin (or FB1). Left panel (C17.2 cells): lane 1, ceramide standard (St); lane 2, control (Con) cells; lane 3, myriocin (myr)-treated cells. Right panel (ES cell-derived NPs): lane 4, ceramide standard; lane 5, control NPs; lane 6, myriocin-treated NPs; lane 7, FB1-treated NPs. **C.** Quantification of the number of migrating NPs. Note that myriocin treatment reduced the number of migrating NPs by more than 90%, which was partially reversed by 40 μM S18 or 20 μM LiCl. All quantitative results are means obtained from at least n = 3 independent experiments, lines on bars represent the standard deviation, **P*<0.05; ***P*<0.01.

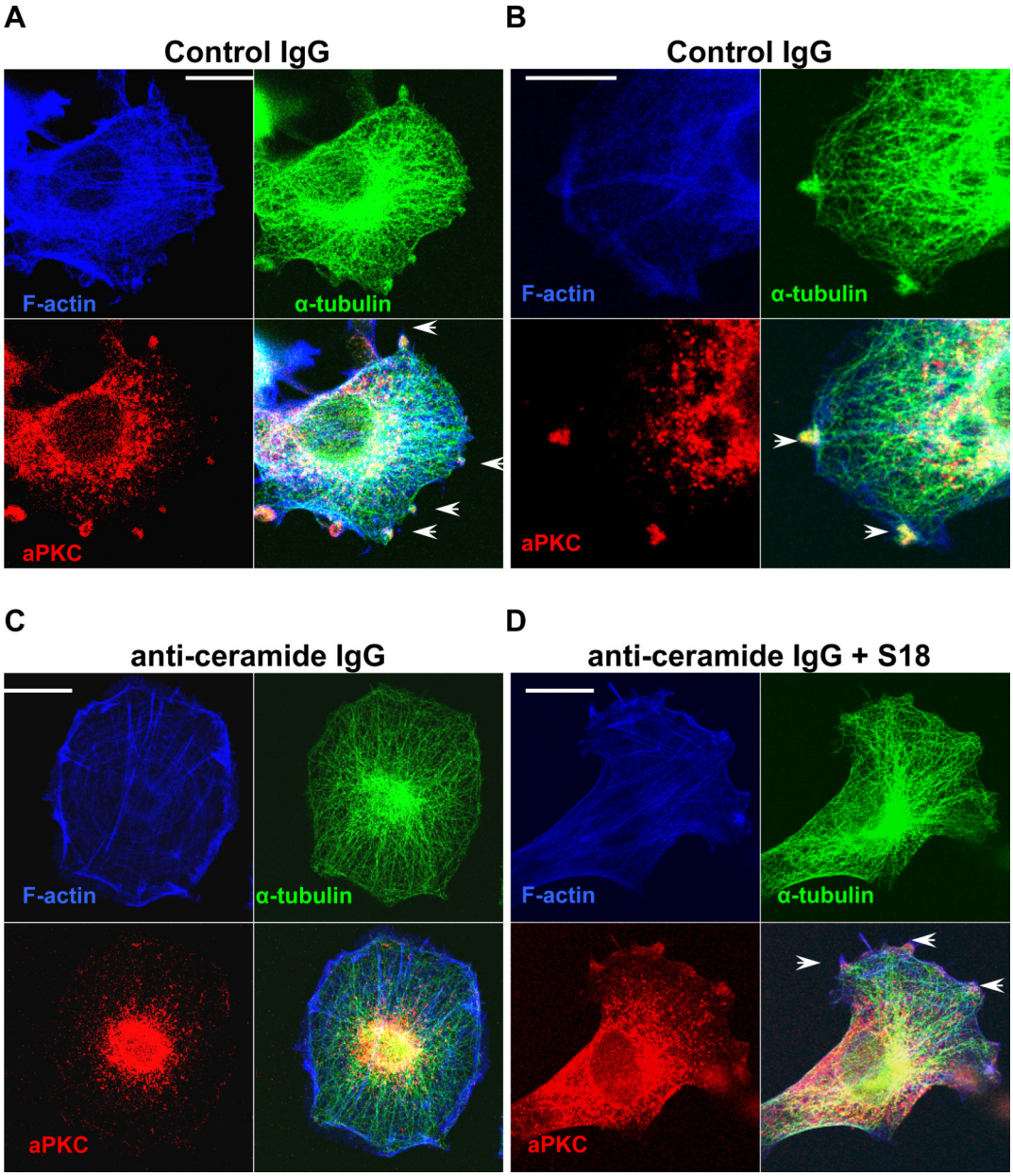

Fig. 2. Anti-ceramide antibody induces distribution of membrane-bound aPKC to the cytosol and obliterates microtubule extension to the membrane

A. Control IgG (pre-immune serum). Endogenous aPKC (red) and α-tubulin (green) was detected using the respective antibodies. F-actin was stained with Alexa 647-conjugated phalloidin (blue). Note that aPKC and the plus ends of microtubules were co-localized at membrane protrusions. A similar distribution was observed with anti-GA1 or anti-FGFR1 rabbit IgG used as additional control antibodies. **B**. Same as in A, but at higher magnification. **C**. Same as in A, but after incubation with anti-ceramide rabbit IgG (20 μg/ml protein A sepharose eluate) for 4 h. Note that aPKC was distributed to the perinuclear region and microtubules did not extend to membrane protrusions. **D**. Same as in C, but simultaneous addition of 40 μM S18. Bars in A-D = 5 μm

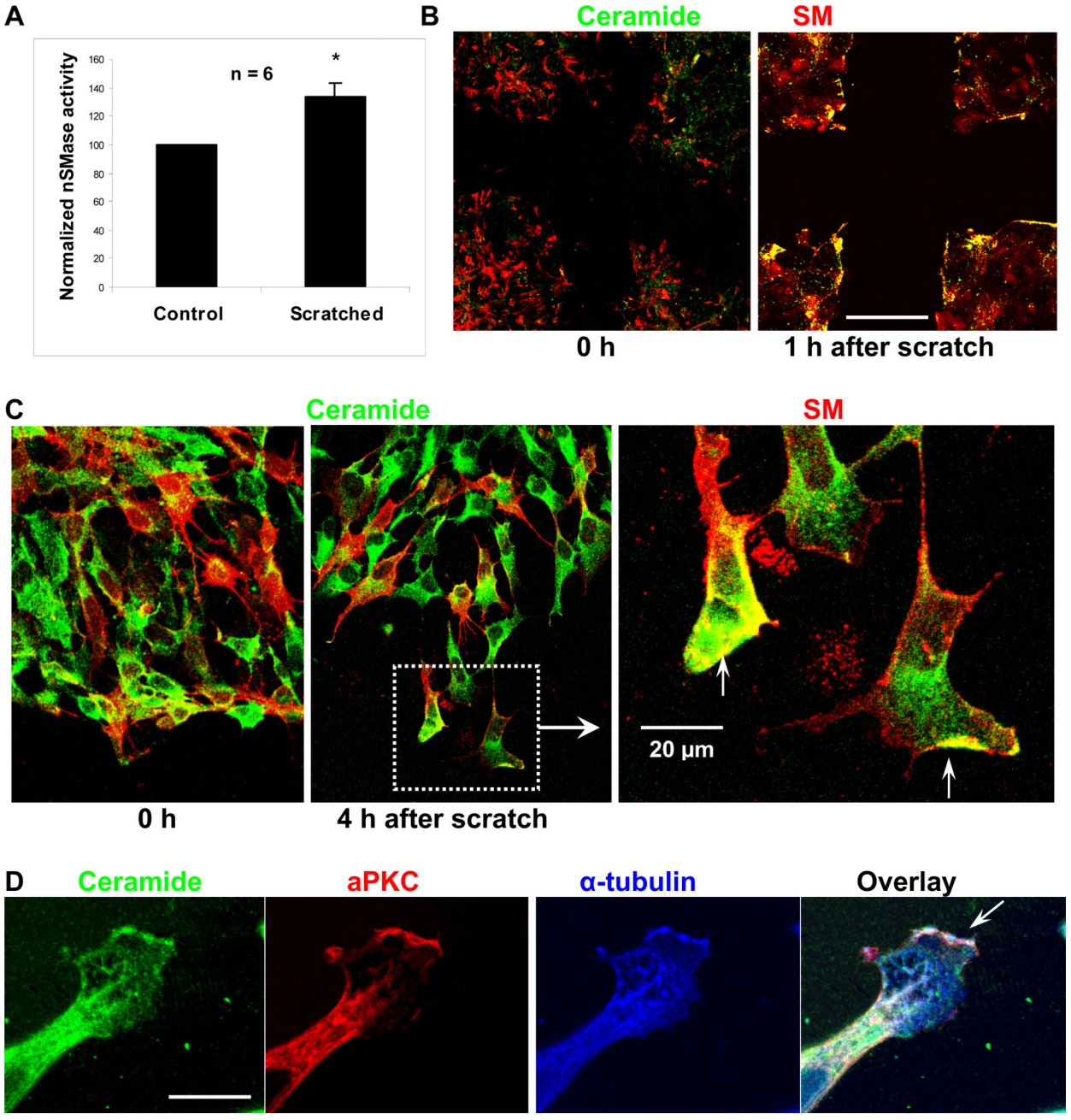

Fig. 3. SM-derived ceramide is distributed to the tip of processes and the leading edge of migrating cells

A. Activity of nSMase as detected by the Amplex Red assay one hour after wounding of a C17.2 monolayer in a scratch migration assay. **B**. Immunocytochemistry using antibodies against ceramide (green) and lysenin (red), a protein specifically bound to SM microdomains. Note elevation of ceramide at the edges of the wounding gap as determined one hour after generating the scratch. Bar in B = 200 μm. **C**. Scratch migration assay followed by immunocytochemistry for ceramide and SM (red) at higher magnification. Bar in C = 20 μM. **D**. Immunocytochemistry for ceramide (green), aPKC (red), and α-tubulin (blue). Note that ceramide, aPKC, and α-tubulin were co-distributed to the leading edge of

the membrane process. See also Supplemental Fig. 3B for FRET analysis (ceramide-to-α-tubulin FRET signal). Bar = 5 μm.

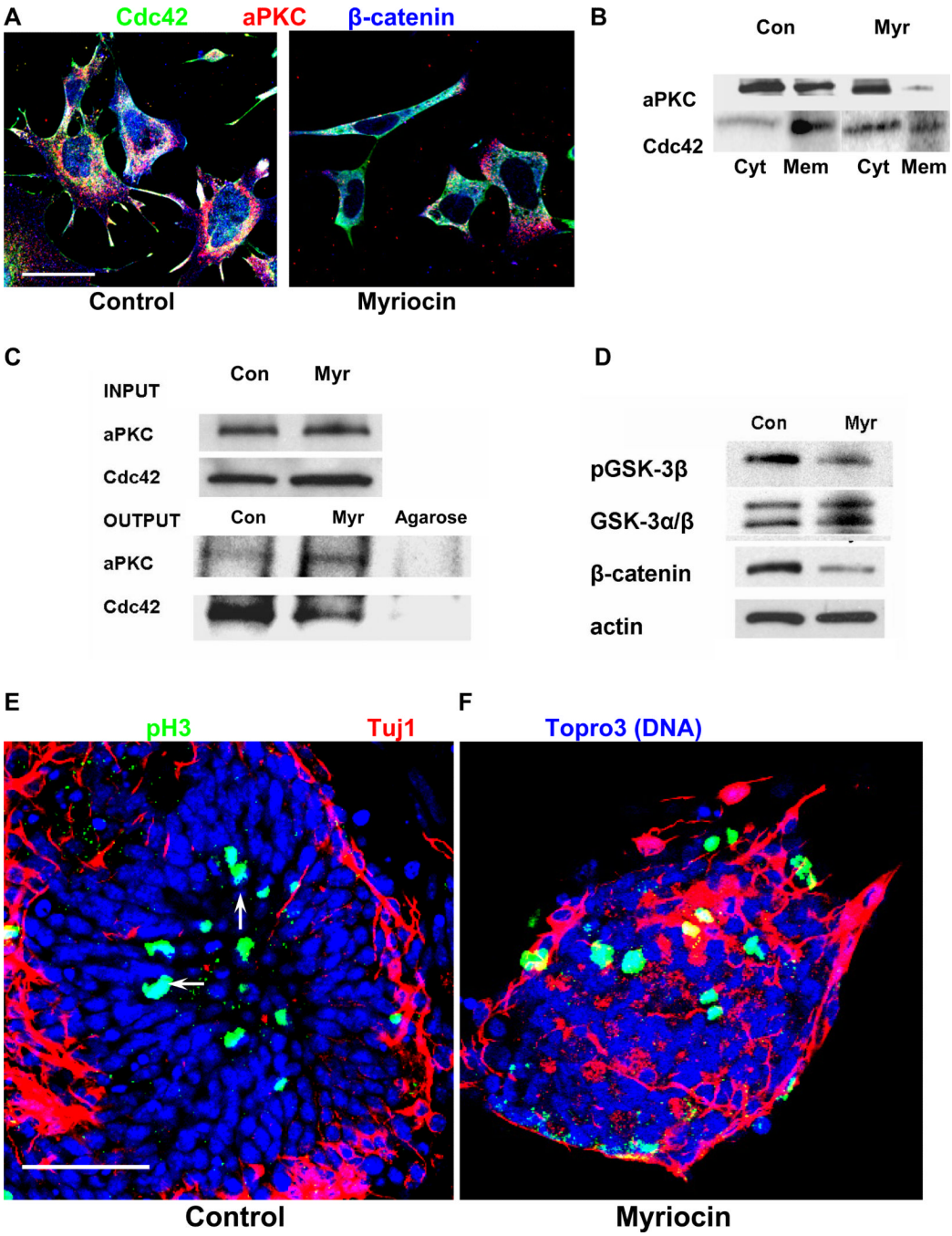

Fig. 4. ***Ceramide regulates the interaction of* aPKC *with Cdc4 and polarity in NPs***

A. Immunocytochemistry using antibodies against Cdc42 (green), aPKC (red), and β-catenin (blue) with ES cell-derived NPs. Note that myriocin treatment obliterated the co-distribution of Cdc42, aPKC, and β-catenin in membrane protrusions, and prevented the translocation of β-catenin to the nucleus. Bar = 5 μm. **B**. Subcellular fractionation assays separating the membrane and cytosolic fraction of NPs. Immunoblotting was performed using antibodies against PKCζ/λ and Cdc42. Note that myriocin treatment reduced the membrane distribution of these proteins. Cyt, cytosol; mem, membrane fraction. **C.** Protein was solubilized from NPs and co-immunoprecipitation assays performed using an anti-PKCζ/λ antibody for the precipitation reaction and a Cdc42 antibody for the immunoblotting reaction. Myriocin

treatment reduced the amount of co-immunoprecipitated Cdc42 by more than 70%. The upper panel is the loading (input) control confirming that the same amount of endogenous protein (aPKC, Cdc42) was used for the immunoprecipitation reaction with control and myriocin-treated NPs. The lanes labeled “Agarose” show the results of the co-immunoprecipitation reaction using Protein A agarose without antibodies (negative control). The absence of protein immunostained in the blotting reaction confirms that binding was specific for the (co)immunoprecipitated antigen. **D**. Myriocin treatment reduced phosphorylation of GSK-3β and the β-catenin protein level in myriocin-treated NPs. **E, F**. Myriocin treatment caused ectopic localization of mitotic NPs. In control cells, pH3(+) NPs were localized in the center of the concentric rosettes (arrows). In ceramide-depleted cells, the distribution of mitotic and post-mitotic cells was disorganized. Rosette formation was reduced by more than 90%. Nuclei were stained with Topro-3-iodide and pseudo-colored in blue. Bar = 50 μm. The data presented are representative for n = 4 independent experiments.

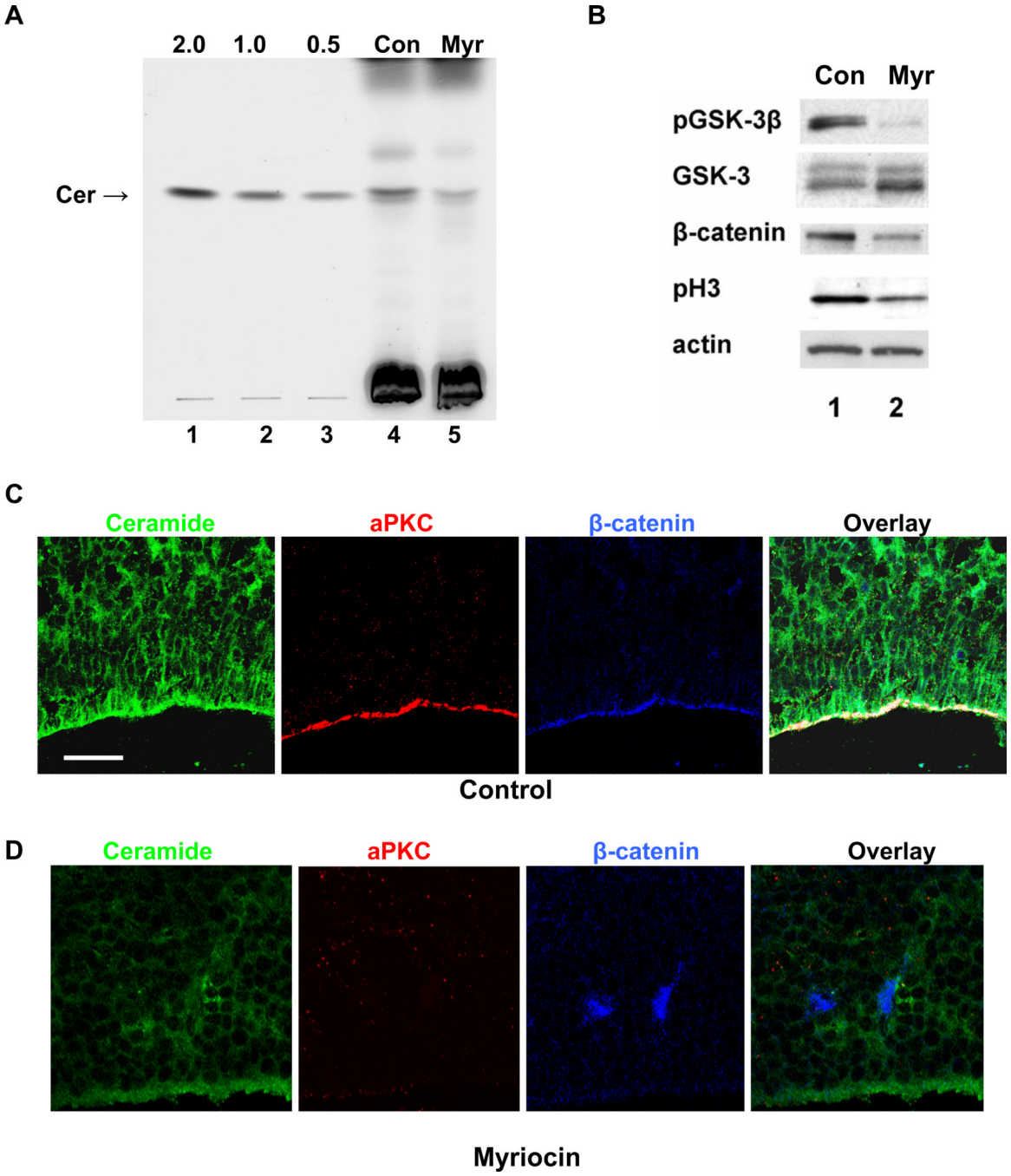

Fig. 5. Ceramide regulates cell polarity in the proliferative neuroepithelium of embryonic mouse brain

A, HPTLC analysis of ceramide levels from whole embryos at E16.5 after injection of myriocin into pregnant mice. The ceramide level was reduced from 2.0+/−0.3 to 0.8+/−0.2 μg/mg cell protein (n=3 experiments). Lanes 1-3, C16 ceramide standards (2.0, 1.0, 0.5 μg); lane 4, control embryos; lane 5, embryos from myriocin-treated mice. **B**. Immunoblotting of protein prepared from embryonic mouse brain. Myriocin treatment significantly reduced phosphorylation of GSK-3β and histone 3, and protein levels of β-catenin in embryonic brains. **C**. Immunohistochemistry (laser scanning confocal microscopy) using sagittal cryosections from E16.5 mouse brain and antibodies against ceramide (green), PKCζ/λ

(red), and β-catenin (blue). Ceramide was enriched in the apical cell membrane of neuroepithelial cells and co-distributed with aPKC and β-catenin (color white in overlay). This distribution was abolished by myriocin (number of mice = 4 in each group; number of embryos = 12 in each group). Also note the complete loss of aPKC and β-catenin in the apical membrane, and the disappearance of the pseudostratified morphology of cells in the neuroepithelium. Bar = 50 μm.

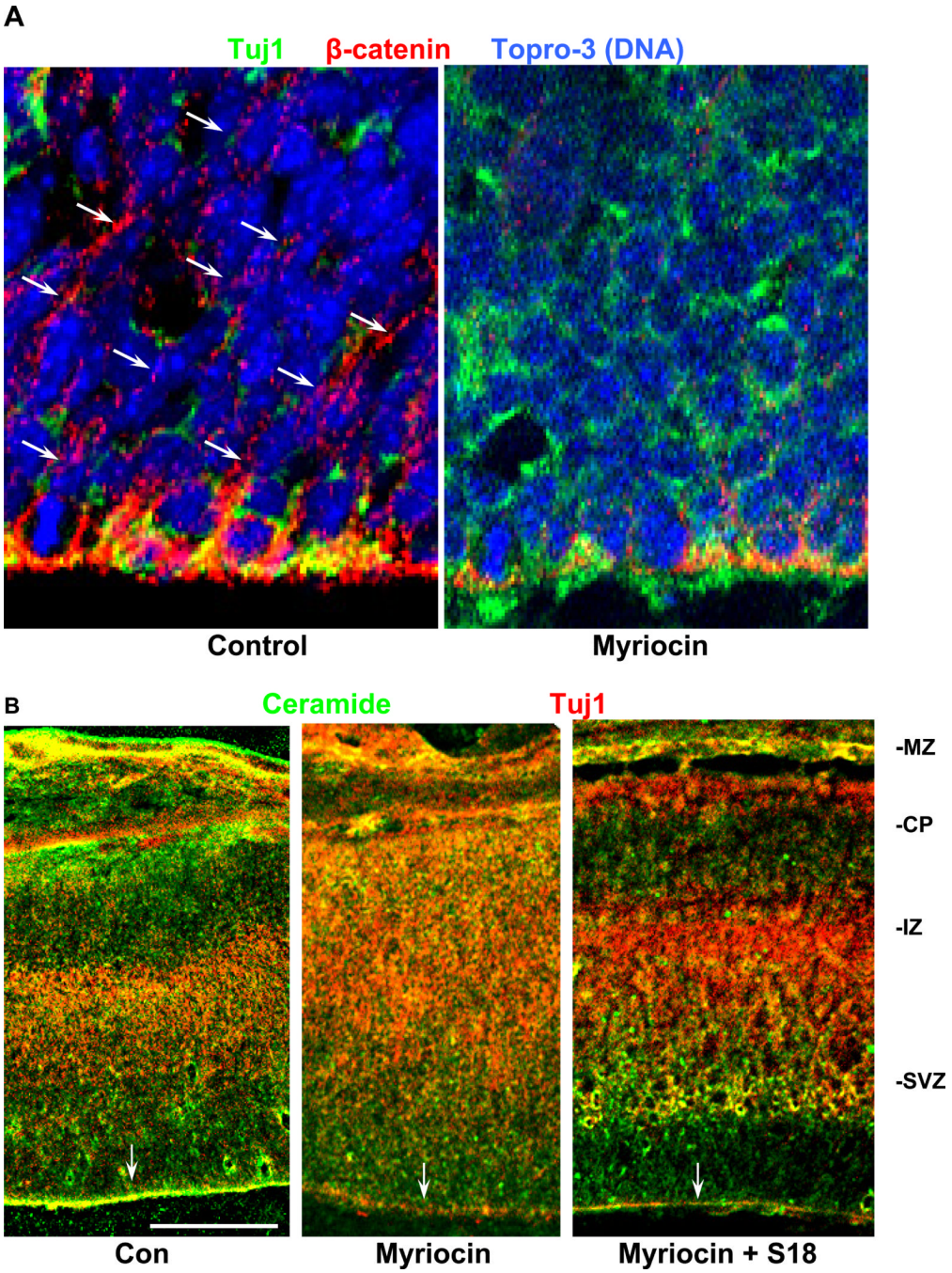

Fig. 6. Ceramide regulates the distribution of NPs and neuronal precursors, and the cortical layer formation in embryonic mouse brain

A. Immunohistochemistry (confocal laser scanning microscopy) using sagittal cryosections of E16.5 embryonic mouse brain and antibodies against β-catenin (red) and Tuj1 (green). Nuclei were stained with Topro-3 and pseudo-colored in blue. Note that myriocin treatment caused (1) loss of β-catenin in the apico-lateral membranes, (2) rounded up and non-aligned (randomly distributed) cells, and (3) ectopic localization of Tuj1(+) cells. **B.** Overview on sagittal sections of E16.5 embryonic mouse brains. Immunocytochemistry was performed using antibodies against ceramide (green) and Tuj1 (red). Note that the border between the intermediate zone (IZ) and the cortical plate (CP) was no longer visible in myriocin-treated

embryos. S18 restored the wild-type phenotype without elevating ceramide in the apical membrane. MZ, marginal zone. Bar = 200 μm.

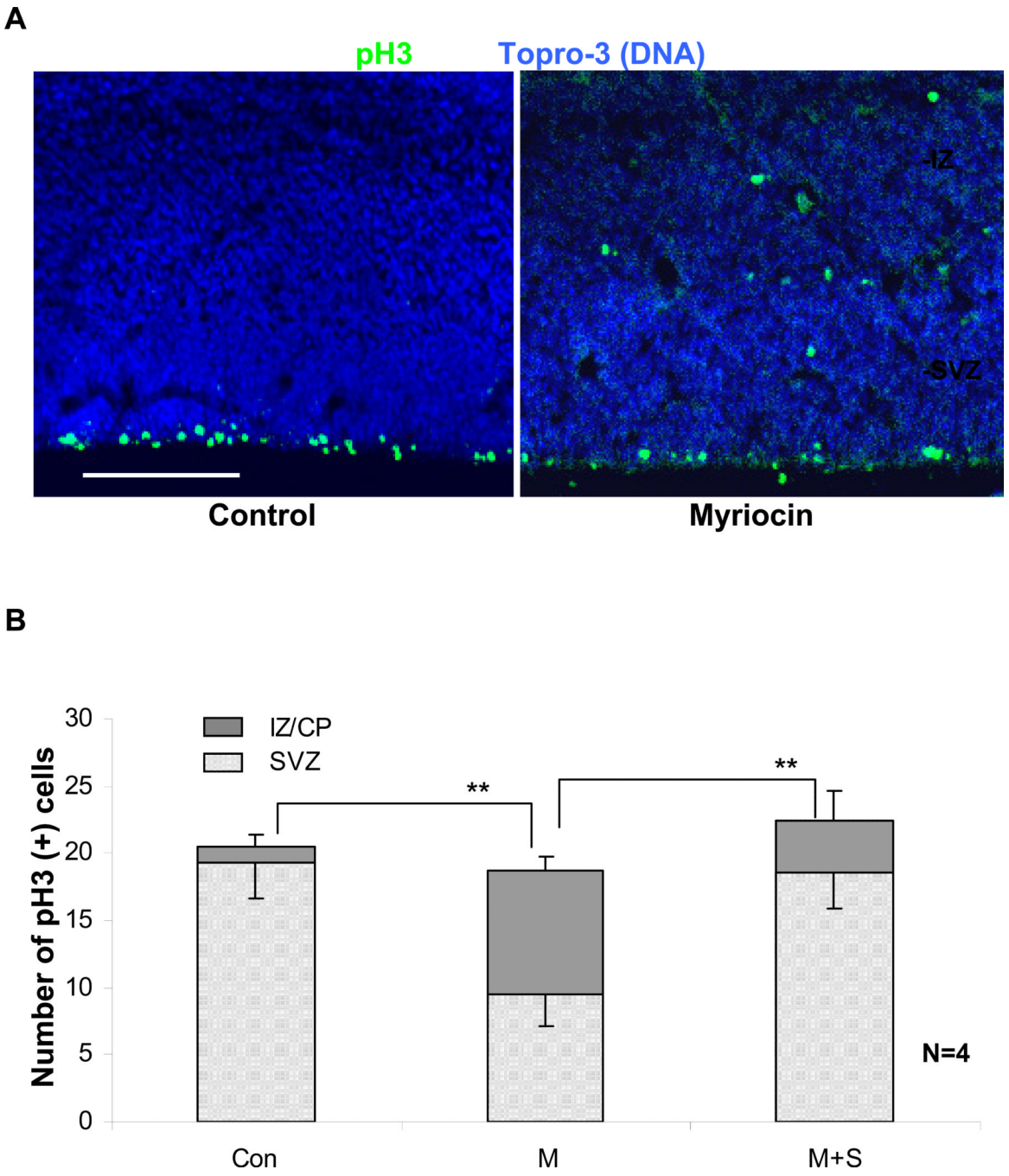

Fig. 7. Myriocin treatment causes ectopic localization of mitotic NPs

A. In control embryos (left), mitotic NPs (pH3(+)) were strictly confined to the VZ/SVZ. In myriocin-treated embryos (right), mitotic NPs were ectopically distributed throughout all layers of the brain. This result was consistent with the *in vitro* data (Fig. 4E). Bar = 100 μm.

B. Quantitative analysis of the ectopic localization of mitotic NPs. (counts in bins of 200 μm width; n=4 independent experiments, bars and lines on top of the bars represent means and standard error of the means; ** denotes statistically significant differences with $P<0.01$. Number of mice = 4 in each group; number of embryos = 12 in each group.